Discover Geoscience

Research

Clay mineralogy in mylonite weathering products from Njimom (west Cameroon): origin and terracotta suitability

A. N. Nzeukou[1] · D. Tsozué[1] · I. Y. Bomeni[2] · J. R. Mache[3] · M. R. Kwopnang[4] · N. Fagel[4]

Received: 4 July 2024 / Accepted: 23 September 2024
Published online: 03 October 2024

Abstract
This study investigated the mineralogical assemblage of weathering products developed on mylonite rocks in west Cameroon. Smectite and vermiculite occurrence was studied, particularly to emphasize its origin and the potential of the samples in terracotta production. Samples characteristics were determined through X-Ray Diffraction (XRD) and X-ray Fluorescence (XRF) methods. Weathering products were observed along road trenches of 450 m long and 50 m height on a syenitic basement rock intruded by magmatic rock veins. Clay minerals are mainly composed of kaolinite and illite. 2:1 swelling clay minerals (vermiculite, montmorillonite) occur in some samples mainly originated from the contact between weathering materials and quartzo feldspatic bands. The main oxides are SiO_2 (46–72%), Al_2O_3 (16–31%), Fe_2O_3 (2–16%) and K_2O (0.1–6%). Vermiculite may be formed by fluid-mineral interactions during alteration of the chlorite in the plasmic microsystems of the soil. Structural changes in the upper part of the saprolite leading to the transformation of vermiculite into smectite under supergene alteration control, which predominates in humid tropical zones. Heavy rainfall leads to the formation of kaolinite at the expense of 2:1 clay minerals. Empirical classification revealed that the studied weathering products can be used to produce common bricks.

Keywords Chemical weathering · Secondary minerals · Clay minerals · Construction material

1 Introduction

Major processes for soils formation at the surface of the Earth are controlled by climate and local factors during weathering and pedogenesis [1–3]. The soil behaviour depends on the type and amount of minerals present therein [4]. Weathering products are observed on trenches along the main road that cross the Njimom locality, near Foumban, in western Cameroon. The properties of these products depend on their particles amount, size, shape, arrangement and mineral composition. These characteristics are well known to result from the disintegration of parent rocks in situ and differ according to the nature of the basement, climate and topography. Clay minerals are among the most abundant constituents derived from this process, and their mineralogy is related to pedogenetic processes [5–7]. Depending on the weathering conditions, some preexisting clay phases may be transformed into other species through a sequence of intermediate interstratified phases. Smectites, for example, in humid climatic conditions, may transform into mixed-layer

✉ A. N. Nzeukou, nzeuk@yahoo.fr; D. Tsozué, tsozudsir@yahoo.fr; I. Y. Bomeni, isaacbomeni@yahoo.fr; J. R. Mache, jamache@yahoo.fr; M. R. Kwopnang, nsmart@live.fr; N. Fagel, nathalie.fagel@uliege.be | [1]Department of Earth Sciences, Faculty of Sciences, University of Maroua, P.O. Box 814, Maroua, Cameroon. [2]Department of Civil Engineering, Fotso Victor University Institute of Technology of Bandjoun, P.O. Box 134, Bandjoun, Cameroon. [3]Department of Mining Engineering, School of Geology and Mining Engineering Meiganga, P.O. Box 115, Meiganga, Cameroon. [4]AGEs, Laboratory of Clays, Geochemistry and Sedimentary Environments, Department of Geology, University of Liege, Allée du 6 Août 14, Quartier Agora, 4000 Liège, Belgium.

kaolinite-smectite (K-S) clays, while vermiculite or mixed-layer chlorite/vermiculite (Ch-V) may result from supergene solutions on biotite or phlogopite or the transformation of chlorite present in the parental rock [8–11]. Many authors evidenced the supergene origin of vermiculite. Some conclusions coming from the study of Basset [12] and revealed that the pegmatitic intrusive zone is mainly formed by producing alkali and silica-rich solutions, favouring then the formation of mica than the vermiculite. Experimental results concluded that the presence of vermiculite in this peculiar area is due to an alteration of the mica, because the presence of a low concentration of potassium generally inhibits the formation of vermiculite. Also, Basset [12] evidences that vermiculite occurrences can be divided in 2 categories, i.e. macroscopic or microscopic (or clayey) vermiculite. Major commercial deposits belong to the first category whereas the material that is mined correspond to mixed-layer vermiculite-biotite or vermiculite-phlogopite. Microscopic vermiculites may be either trioctahedral or dioctahedral with variable compositions and cation exchange capacities, making them difficult to distinguish from smectite [10, 12]. According to Courshesne et al. [13], the formation of smectite depends of the geochemical conditions prevailed in the alteration environment (dissolved base cations and Si concentrations), also by the climatic conditions dominated by a prolonged dry period after a rainy season. The transformation of mica and chlorite during supergene process is believed the most probable mechanism of smectite formation, and this mechanism particularly take place in the interlayer region of these minerals [10, 14]. The difference between smectite and vermiculite is referred to the composition of their interlayer charge, largely located in the tetrahedral sheet. Both are expandable minerals, but the higher layer charge of vermiculite restricts its expansion [14]. Schulze [7] reported that the weathering of micas to vermiculite or smectite can occur after substitution in the interlayer space, K+ by hydrated exchangeable cations. According to Barshad (1966) in [5], the occurrence of vermiculite in a given region is more influenced by climatic factors than the nature of the parent material. Under humid tropical environment like the Njimon area favored by most intense chemical weathering, deep and well differentiated weathering products are observed in comparison of profile observed in the dry tropical climate [15]. Soil profile is an ABC type differentiated from the bottom to top as follow: (i) coarse saprolite with preserved bedrock structure, (ii) fine saprolite with many isalteritic relicts, (iii) nodular horizon with fine red clayey materials containing about 40% of nodules, (iv) set of red clayey and loose horizon with surficial humiferous horizon and rare nodules. The soil profile is resulting of lateralisation process, characterized by intense leaching of the alkaline, alkaline earth elements and some silica of the parent rock. In the mineralogy view, kaolinite is the dominant neo-formed clayey mineral and its presence in the saprolite marks the more advanced stages of weathering [1, 15]. Iron and aluminium sesquioxide (goethite, gibbsite) reflected the intensive tropical weathering (good drainage). The Northern most dry tropical part with low rainfall shows dark grey soils with neoformation of beidellite which transforms upwards into montmorillonite and kaolinite under poor drainage [15].

Clay minerals are used as raw materials in different industries, and their uses and properties depend on their structure and mineralogical composition. Some domains of valorization include ceramic, pharmaceutical or oil industries [16–18]. Studies carried out in Cameroon show clay deposits of various origins (i.e., sedimentary, residual and alluvial) [19–21]. In west Cameroon, notably around Foumban, many potential kaolin deposits, smectite and other clay minerals varieties have been developed as residual products over large areas, resulting in large volumes of weathering products. Previous works with respect to the valorization of these resources have shown that clayey materials from Mayouom and Koutaba (around Foumban) and those from Lembo and Balengou are rich in kaolinite and can be used in refractory industries [22, 23]. There are also numerous clayey deposits for the manufacture of earthen bricks in the localities of Koutaba, Bamendjing, Marom, Mambain and Ndop [23, 24]. Given the importance of the clayey materials resources in the Foumban region on the one hand and the problems related to construction materials encountered by the population on the other hand, the terracotta products sector is interesting for economic development in the country. In this paper, we investigate the main products of weathering mylonite rocks in Njimom (near Foumban) to better characterize them and identify the origin of vermiculite and smectite present inside, and the suitability of these raw materials for terracotta production.

2 Geographical and geological setting

The Njimom area is located on Foumban Shear Zone, part of the Central Cameroonian Shear Zone with mylonitic rocks, mainly calc-alkaline orthogneisses marked by shearing evolution, it is ~ 30 km from Foumban (Fig. 1). The geology of Njimom consists of soil profiles developed on Neoproterozoic mylonite rocks (500–660 Ma) intruded by more recent magmatic veins (40 Ma) [19, 25]. Minerals within the mylonitic band are crushed, flattened or stretched [25]. They are composed of quartz, K-feldspar, plagioclase, pyroxene, amphibole and biotite and the transformation of those primary minerals during the mylonitisation are described by Njonfang et al. [25, 26] as follow: K-feldspar to microcline, plagioclase

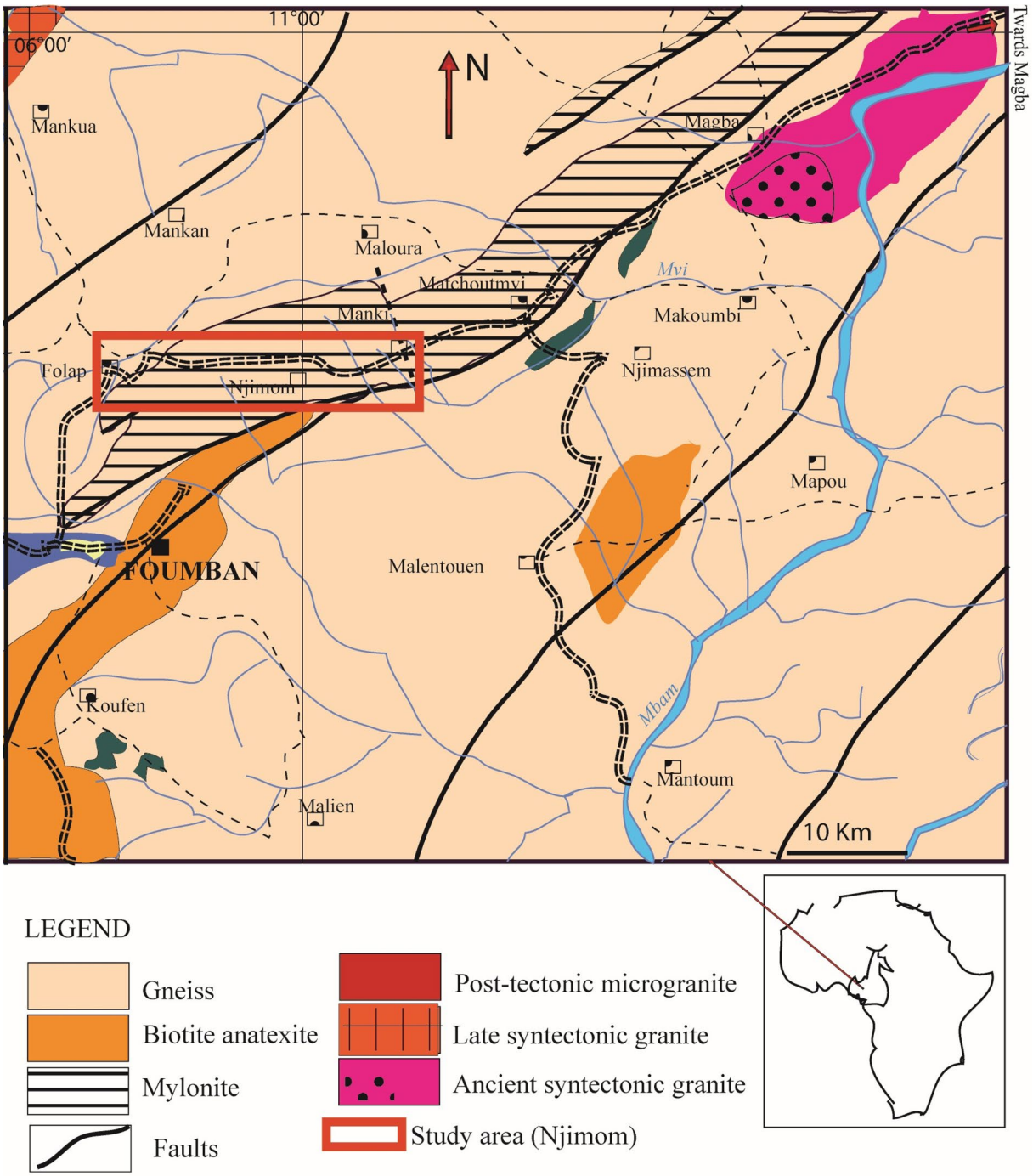

Fig. 1 Geological map and location of the study area (after [51])

to damourite and calcite, pyroxene to amphibole, amphibole to biotite or chlorite, biotite to chlorite or muscovite, sphene to oxides, calcite or epidote. Njoya et al. [23] studied the genesis of kaolin in Mayouom (~ 3 km from Njimom) and revealed that 2 majors processes influenced the weathering evolution of these mylonitic rocks and, are responsible for the weathering products (kaolin) derived: (i) the kaolin indices originating from a hydrothermal alteration and, (ii) the kaolinitic clays originating from a supergene weathering. The study area is tropical characterized by two contrasted seasons: a short dry season (November to February) and a long rainy season (March to October). The mean annual air temperature varies between 22 to 25 °C and the annual average of precipitation is between 1850 to 200 mm per year [23].

3 Material and methods

3.1 Sampling techniques

Field prospection was performed on newly cut road trenches in the locality of Njimom (Fig. 2) between the villages of Manki (east) and Folap (west). From east to west, five levels were chosen on the four trenches described, and in some trenches, only one or two levels were observed (Table 1). The sampling nomenclature was chosen as follows: T1A1 = sample 1 from level A of trench 1. Overall samples are collected based on the colour, texture and recurrence. The general feature of the Njimom weathering sequence developed on the syenitic bedrock is well observed in Trench 2 and may be described as follow: (i) the saprolite horizon marked by the presence of quartzo-feldspathic bands with same orientation as we see in the mylonite, (ii) the fine saprolite horizon with relicts, which may be correspond to A, B and C levels, and (iii) the fine clayey horizon which may be correspond to D and E levels.

Trench 1 (~ 300 m long and 40–50 m high, close to Manki) has 5 levels labelled A to E with no clear vertical variation and the mylonitic bedrock is not appear here (Fig. 2). In lateral variation, increasingly fine materials are observed with, in places, intersections with quartzo-feldspathic bands. At level A, the height reaches 10 m, and there is no major difference from the materials at levels B and C. Based on some structures and materials observed, this trench presented an interest centre: the chemical and mineralogical composition of the contact zone between the quartzo-fedspathic bands and the surrounding clayey material. 5 samples were collected at level A following lateral variation and one at level D (Table 1).

Trench 2 (50–60 m high) shows a soil profile developed on mylonitic rock. The bedrock presented parallel debitage plans consisting of an alternation of white quartzo-feldspathic banks and dark ferromagnesian mineral-rich banks. Three outcrops appeared along the 450 m long wide trench. Compared to trench 1, this trench features lateral and vertical variations in facies, similar to what has been found in many weathering patterns in tropical areas. The grain size decreases upward as one moves away from the parent rock (mylonite). The lateral variation is marked by an alternation of facies of different colors with more clayey material upwards. The quartzo-feldspathic bands observed along the weathering profile maintain the orientation of the bedrock but are less common upwards. Since the material was homogeneous in grain size, three samples were collected on the E based on the color of the clayey material. Njonfang et al. [26] described the geochemistry data of these mylonitic bedrock which consist of SiO2 (56 to 74.5%) with the sum of alcalin between 6 to 40%. They belong to the Middlemost transalcalin domain, and trace elements are more abundant in dark facies

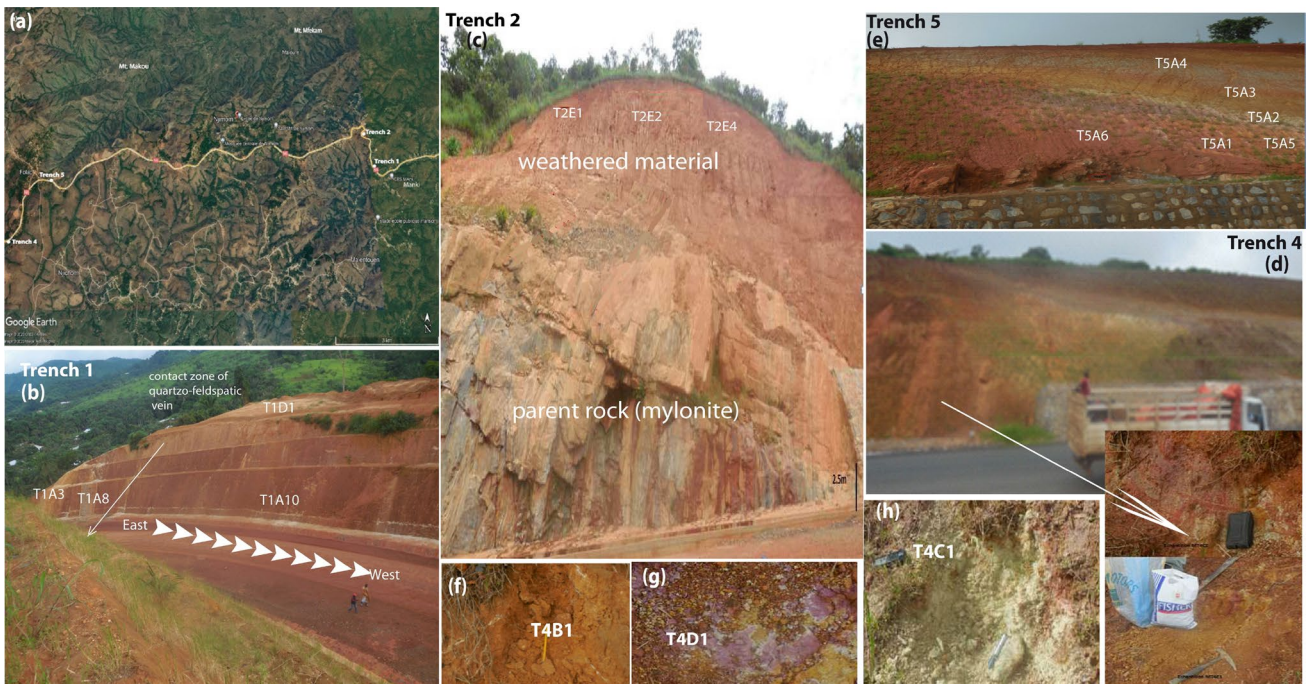

Fig. 2 **a** Location of trenches (Google Earth, 2023); **b**–**e** Location of some sampling points on trenches, **f**–**h** are samples marked by differentiated color in trench 4

Table 1 Lithological description of sample materials from Njimom area (west Cameroon)

Labels	Altitude	Lithological description
Trench 1 (~300 m long and 40–50 m height) N05° 49.440; E11° 00.439		
T1A1 (0–8.8 m)		Yellow to greenish compact clay with shale structure; we were observed traces of black colour that seem to form along the weakness planes
T1A3 (8.8-10 m)		Compact lightly-yellowish clay with shale structure marking the transition between soil and quartz-feldspathic vein; also observed on the right side of the trench, with an orientation N065° E
T1A8 (10–40.7 m)		Compact reddish-yellowish sandy clay with many centimetric veins of quartzo-feldspar
T1A10 (40.7–89.1 m)		Compact yellowish sandy clayey material with reddish spots
T1A11(89.1–216 m)		Yellowish silty clayey with whitish and pinkish spots
T1D1 (~10 m long)		Whitish clay
Trench 2 (~450 m long and 30 m height): N05° 50.018′, E11° 00.083′		
T2E1		Reddish sandy clayey material
T2E2		Yellowish sandy clayey material
T2E4		Yellowish sandy clayey material
Trench 4 (~250 m long and 30 m height): N05° 49.763′; E010° 55.951′		
T4B1		Lightly yellow to orange clay
T4C1		Whitish clay layer of 2 m thick
T4C2		Multicolour clay (white. grey. purple and red) of 1.5 m thick
T4D1 (~3 m height)		Purple compact clay layer of 1 m thick
T4E1(~10 m height)		Yellowish clay layer of 2 m thick
Trench 5 (~200 m long and 30 m height): N05° 49.554′; E10° 56.623′		
T5A1		Pinkish clay
T5A2		Lightly grey clay
T5A3		Yellowish clay
T5A4		Dark grey clay
T5A5		Orange clay
T5A6		Dark pink clay

than in whitish one. The variation of proportion of transition element reflects the relative abundance of ferromagnesian minerals which fractionate them [26].

Trenches 4 and 5 show several clayey layers with different colors (ochre, white, multicoloured, mauve or red) over approximately 30 m. These clayey layers are homogeneous in terms of color and grain size.

Trench 4, located ~ 8.2 km from trench 2, extends ~ 250 m long and 30 m high over four levels (B, C, D and E). At level B, a clayey material with an orange—yellow color was observed at the two lateral ends of the trench. At level C, the composition is similar to that observed at level B. A pure white clay band ~ 2 m thick (T4C1), observed at the western end, lies on a succession of 1.5 m thick clayey layers of different colors, giving rise to a particular feature (T4C2). The D level (~ 3 m in height) consists of a mauve-colored very plastic clay (T4D1). At level E, a clayey-sandy material (~ 10 m height) with a dark red color was observed, ending in its eastern part with a compact clayey band that was yellow in color with mauve spots (T4E1).

Trench 5 is located 1 km east of trench 4, extends 200 m long and has only one level (A). The clayey materials observed here present the same variety of colors as trench 4.

A total of twenty samples (Table 1) was characterized in the laboratory by X-ray diffraction and X-ray fluorescence spectroscopy.

3.2 Analytical methods

X-ray diffraction (XRD) was carried out on randomly oriented powders and on oriented aggregates using a Bruker Advance D8 ECO diffractometer (Cu Kα1 radiance, λ = 1,5418 Å, 40 kV, 30 mA) in the laboratory AGEs (ULiège, Belgium) according to the methodology of Moore and Reynolds [27]. Small powdered sample (grinding less than 80 µm) were deposited on sample holder by front loading to reduce the preferential orientation. The < 2 µm fraction were separated by settling in a water column; after samples were mounted as oriented aggregates on glass slides and three X-ray patterns were recorded on each sample: air drying (24 h), glycolation (24 h) and heating (500 °C for 4 h). The measurements were carried out in the 2θ range from 2° to 45° with a step size of 0.02° and a time per step of 2 s. Identification of mineral phases was carried out using Bruker®Eva software. The relative mineral abundance was estimated from the patterns using the Rietveld method through TOPAS Bruker software.

The chemical composition was determined by X-ray fluorescence spectroscopy (XRF) with Bruker S8 Tiger 4 kW spectrometer equipment (PGEP, ULiege, Belgium). The chemical index of alteration (CIA) defined by [28] was used to estimate the chemical weathering intensity of the samples.

SEM observations were used on the T1A3 and T4C1 samples to characterize the morphology and the size of the vermiculite and smectites minerals detected by XRD. The observations were made on a FEG-ESEMXL3 type (Greenmat, ULiege, Belgium). The samples were metallized with gold powder by plasma spraying (distance 5 cm, 30 mA, 0.05 atm, Argon, 50 s), and images were subsequently obtained by a secondary electron detector at accelerating voltages of 10 kV and 15 kV. Fourier transform infrared (FTIR) spectroscopy was used in complement to confirm the XRD results obtained from those particular samples. Spectra were recorded between 4000 and 400 cm^{-1} on a Bruker® alpha-P spectrometer on KBr pellets.

4 Results and discussion

4.1 Mineralogical composition of weathering products

Bulk powder diffractograms revealed the intensity of the main peak (with semi-quantitative estimation) characteristic of total clay fraction with a general amount between 10–80%, quartz 5–60%, feldspars (orthoclase < 10% and microcline < 30%), muscovite < 15%, anatase < 20% and hematite < 20% (Fig. 3). The majority of the samples consisted of quartz followed by potassium feldspar. Others species encountered in various proportion are: in trench 1 we note the presence of plagioclase (albite) < 20%, goethite ((5–20%), calcite and dolomite (< 5%), in trenches 1 and 2 the presence of aragonite < 5%, and in trenches 1, 2 and 4 the presence of augite < 5% (Table 2).

The clayey < 2 µm fraction essentially consists of kaolinite (20–80%) and illite (< 10%) in trenches 1 and 5. Other clay minerals species (chlorite, smectite, vermiculite) may be existed in the milieu by observing the behaviour of peaks at: normal condition (N), ethylene glycol (EG) and heated (H) treatment. For example, T1A1 showed a peak at

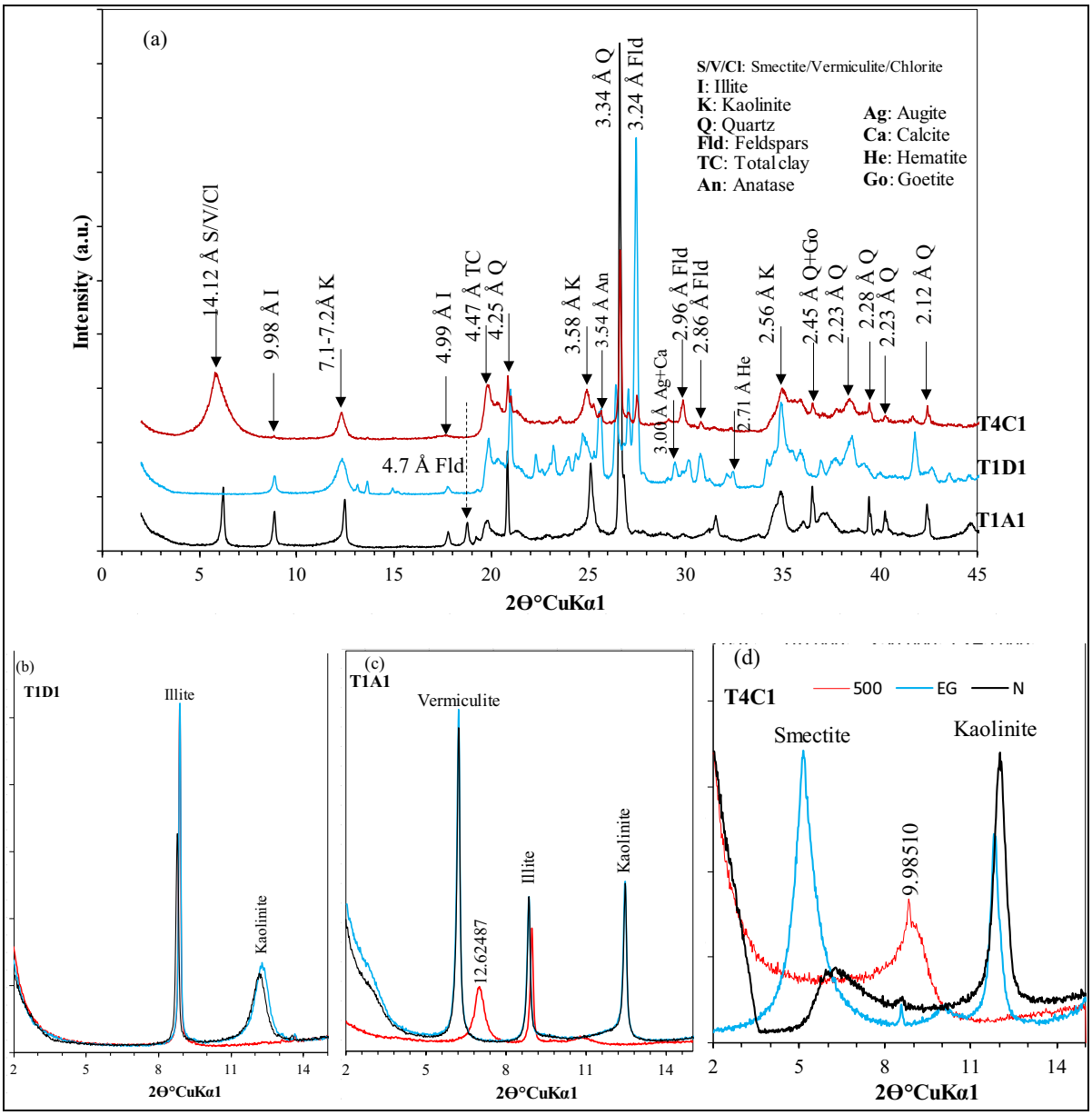

Fig. 3 Specimen diffractograms of some samples. **a** Bulk diffractograms; **b–d** oriented diffractograms (N-natural, EG-ethylene glycol, 500-heated), T1A1 and T4C1 samples respectively contain vermiculite and smectite

14 Å under (N) conditions and after treatment with (EG), and at 12 Å after heating to 500 °C, where the intensity was reduced by half (Fig. 3). According to [5, 29, 30] these peaks may be attributed to chlorite that underwent alteration into vermiculite. The decrease in intensity by half after heating to 500 °C may indicate that it is more likely to be a mixed-layered Ch-V consisted of 50% chlorite and 50% vermiculite [29, 30]. T1A3 taken 3 m from sample T1A1 showed a peak corresponding to N and EG at 14 Å, which moved to 10 Å after heating; this behaviour may be attributed to vermiculite. The semi-quantitative estimation suggests chlorite and montmorillonite (< 10%) in trench 4, vermiculite (< 20%) in trench 1 (T1A1, T1A3). The smectite (montmorillonite) (5–10%) are present in samples T4D1, T4C1 and T4C2. Overall, the methodology used here to evidence vermiculite seem limited, and according to Srodon [14] vermiculite could definitely be confirmed by Mg saturation and glycerol treatment and can be further elucidated through incremental heating (e.g. 330 then 550 or 400 then 550 °C) and EG treatment of Ca saturated samples.

Table 2 Semi-quantitative mineralogical estimation (%)

Sample	Qtz	Augite	Feldspars			Muscovite	Total clay					Oxides			Carbonates		
			Albite	Orthoclase	Microcline		Illite	Chlorite	Montmorillonite	Vermiculite	Kaolinite	Goethite	Hematite	Anatase	Calcite	Dolomite	Aragonite
T1A1	< 30	< 5	< 2	–	–	< 10	–	–	–	< 15	< 25	< 10	–	< 5	–	–	–
T1A3	< 30	< 2	–	–	–	< 2	< 3	< 5	–	< 20	< 20	< 15	–	< 10	–	–	–
T1A8	< 30	< 2	< 2	–	–	< 5	–	–	–	–	< 40	< 10	< 10	< 5	–	–	< 2
T1A10	< 40	< 5	< 20	< 10	–	< 2	–	< 10	–	–		< 5	< 3	< 2	< 2	< 2	< 2
T1A11	< 20	< 2	–	< 10	–	< 3	–	< 2	–	–	< 40	–	< 15	< 5	––	–	< 2
T1D1	< 5	< 5	–	< 10	< 30	< 10	–		–	–	< 35		< 10	< 2	–		
T2E1	< 40	< 3	–	< 10	< 20	< 3	–		–	–	< 20	–	< 5	< 3	–	–	
T2E2	< 30	< 2	–	< 3	< 5	< 5	–	< 3	–	–	< 40	< 2	< 10	< 3	–	–	< 2
T2E4	< 20	< 2	–	< 5	–	< 5	–	< 2	–	–	< 50	< 2	< 10	< 3	–	–	< 2
T4B1	< 30	< 2	–	–	–	< 2	–	< 2	–	–	< 55	< 2	< 3	< 3	–	–	–
T4C1	< 10	< 5	–	–	< 5	< 15	–	< 2	< 5	–	< 30	–	< 20	< 5	–		
T4C2	< 20	–	–	–	< 2	< 15	–	< 3	< 3	–	< 35	< 2	< 20	< 10	–	–	–
T4D1	< 45	< 2	–	–	–	< 5	–	< 2	< 10	–	< 35	–	< 2	< 5	–	–	–
T4E1	< 5	–	–	–	–	–	–	–	–	–	< 80	–	< 2	< 20	–	–	–
T5A1	< 30	–	–	< 2	–	–	–	–	–	–	< 60	–	–	< 10	–	–	–
T5A2	< 10	–	–	< 2	–	–	< 5	–	–	–	< 70	< 2	–	< 15	–		
T5A3	< 20	–	–	< 2	–	–	< 5	< 2	–	––	< 50		< 2	< 15	–	–	–
T5A4	< 15	–	–	< 2	–	–	< 10	–	–	–	< 60	–	–	< 15	–	–	–
T5A5	< 35	–	–	< 2	–	–	< 5	–	–	–	< 50	–	–	< 10	–	–	–
T5A6	< 60	–	–	< 2	< 10	< 5	–	–	–	–	< 20	–	–	< 3	–	–	–

Samples from trenches 4 and 5 present high kaolinite proportion, and their clayey < 2 µm fraction represents 40 to 70% of the composition of the bulk powder (Table 2, Fig. 4). According to Njonfang et al. [25, 26], the presence of chlorite in mylonitic basement rock paragenesis is due to their microtexture and the mineralogical changes that occurred during deep crustal (15–20 km) mylonitisation.

This phenomenon is responsible for the transformation of pyroxene to amphibole, amphibole to biotite or chlorite, and biotite to chlorite or muscovite mostly during interactions with late-stage hydrothermal fluids [25, 31]. In the soil profile, where rock structures are non-preserved and engaged in the supergene alteration process, these chlorites experience secondary alteration plasma microsystem destruction, leading to the formation of vermiculite [1, 2, 31]. The presence of vermiculite is probably related to the location of the sample in the contact zone between the clay mass and the plurimetric quartzo-feldspathic bands.

With regard to the probably presence of smectites, some samples showed a peak at 14.7 Å under normal conditions (N) and 16.6 Å after glycolation before collapsing at 9.9 Å after heating to 500 °C (Fig. 3). Additionally, on FTIR spectra, the stretching vibration frequency of the structural OH group strongly varies as a function of the octahedral cation on which it is in coordination. According to Madejova [32] this band appears at 3620 cm^{-1} (AlAlOH) in montmorillonite (Al-rich smectite) and also in kaolinite. The peak at 3620 cm^{-1} indicates the presence of kaolinite, montmorillonite or both. Moreover, for the analysed sample, absorption bands centred at approximately 1625 cm^{-1} represent OH vibration of water [32, 33]. The absorption bands of the T1A3 sample may be reveal the presence of another mineral species in addition to kaolinite (Fig. 5). These values are slightly different from those of the kaolinite standard peaks (3550 cm-^{1}, 3375 cm^{-1}, 3250 cm^{-1}, 1657 cm^{-1}, 1070 cm^{-1}) [34]. The peaks observed at 3391 cm^{-1} and 3234 cm^{-1} most likely corresponded probably to the stretching vibrations of the OH bonds of the water molecules present between the sheets of 2:1 clay mineral. The bands at approximately 1116 cm^{-1}, 1030 cm^{-1} and 1007 cm^{-1} represent the stretching vibrations of the Si–O bands [34, 35]. At the 830 cm^{-1} band vibration, if Mg substitutes to Al, it may correspond to Mg for Al substitution in the octahedral layer [33–35].

In Fig. 6, EDS spectrum and its respective image reveal the presence of magnesium, potassium and iron in T1A3 sample, calcium and iron in T1C4 sample which may confirmed the presence of vermiculite and montmorillonite in those samples respectively.

Among the chemical elements commonly observed in clay minerals, potassium is more common in mica, Mg might be a marker of vermiculite compared to smectites which contain hydrated cations (Na^{+} et Ca^{2+}) in their interlayer space

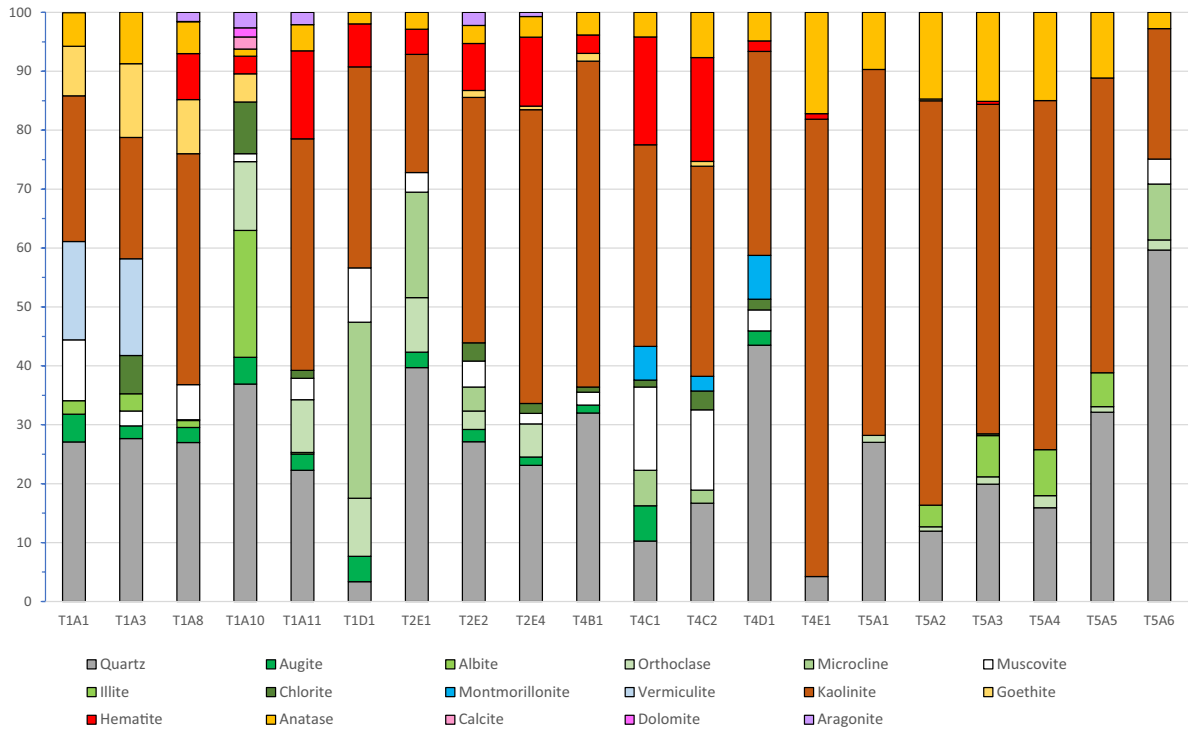

Fig. 4 Mineralogical estimation of studied samples

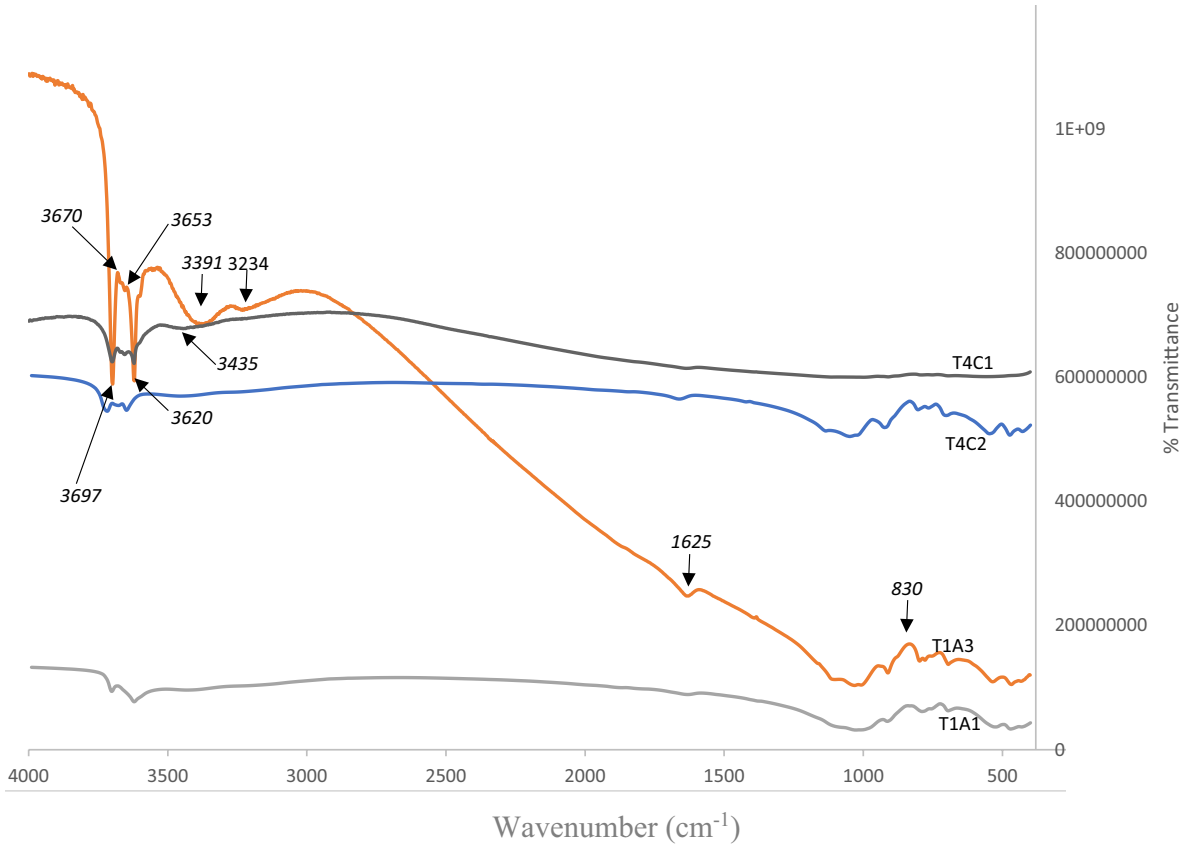

Fig. 5 Infrared spectrum of weathering products containing vermiculite (T1A1, T1A3) and smectite (T4C1, T4C2)

[10, 20, 33]. The common chemical elements obtained in analysed samples are Si, Al, K, Ti, Fe and Mg. Mg content could point to vermiculite and Ca or Na could point to smectite, these results would go towards confirming the postulate explained with XRD results.

The possible provenance of smectites may be the transformation of muscovite present in those weathering products. Many authors have proven that biotite and muscovite, as well as sericites included in some plagioclase grains, can undergo transformation during bedrock weathering to produce smectites [10, 36]. Pseudomorphic transformation of plagioclase produce microgranular material which includes small units' zones where optic characteristics of muscovite are observed [36]. As we know in the literature, smectites are principally found in poorly drained environments, high pH and abundant base cations and they can form from different precursor minerals [37].

In this study, where strong leaching conditions prevailed under warm and humid tropical environments, the presence of smectite in the soil profile may be attributed to a particular environment where fluid-mineral interactions operate inside weathering microgranular materials originated from plagioclase [10, 36]. These smectites derived from di- or trioctahedral micas (muscovite/biotite) are named "transformation smectite" (Robert, 1973 in [36]). The formation of vermiculite by transformation of micaceous minerals is known and described by several authors in temperate climates. In the tropical climate, illite and beidellite- montmorillonite have been reported, vermiculite is not common. The occurrence of vermiculite should be due to particular microsystems conditions in relation with the previous shearing evolution and hydrothermal alteration before weathering of the mylonite (bearing damourite, chlorite, biotite, muscovite) which favors the formation of some 2/1 clays, with kaolinite as the dominant clay mineral [1–3].

Based on the X-ray diffraction results, clay minerals from the Njimom locality can be merged in two categories: trenches 1 and 2 are less rich in kaolinite whereas trenches 4 and 5 are enriched in kaolinite. These clayey materials can be considered as kaolinitic raw clays exploited as refractory material products [18, 23].

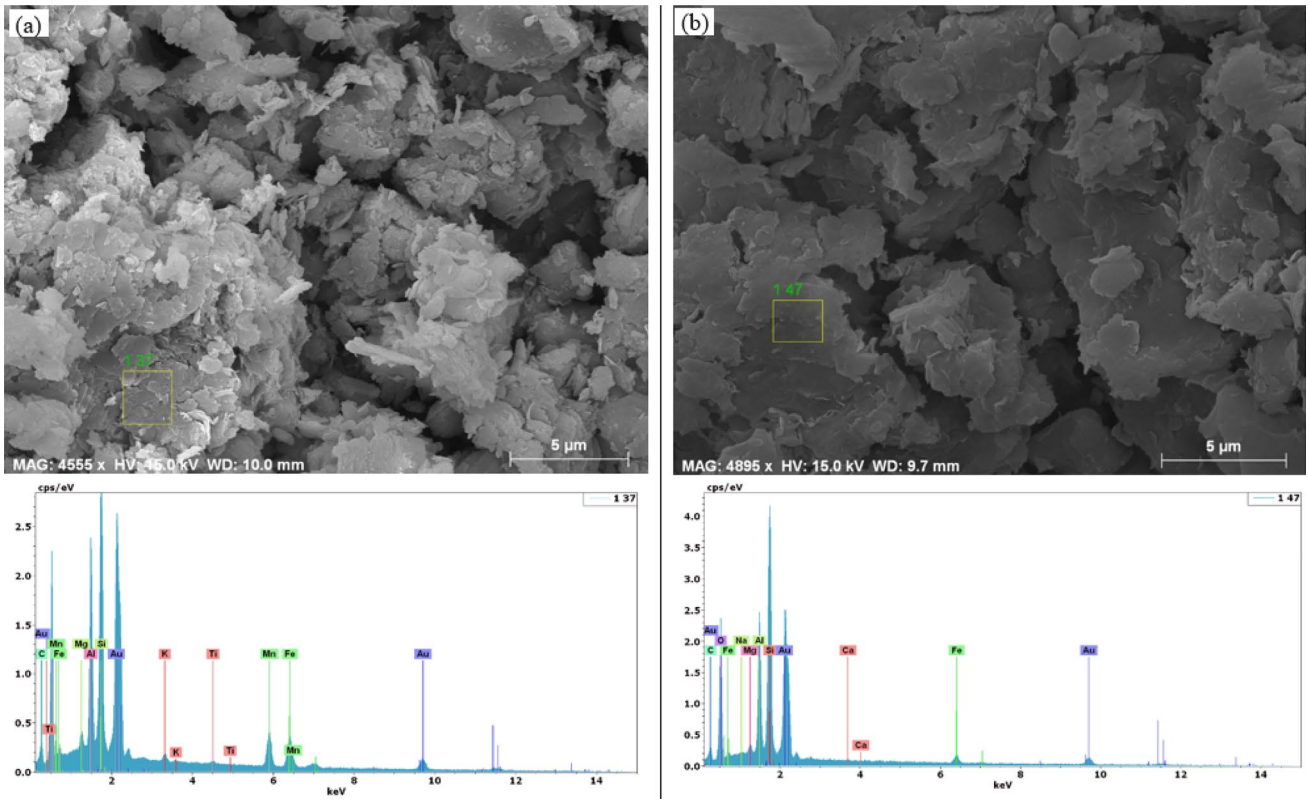

Fig. 6 SEM micrographs of weathering products of T1A3 and T4C1 samples coupled with EDS spectrum of different phases: (**a**) Mg content could point to vermiculite; (**b**) Ca or Na could point to smectite

4.2 Geochemistry of the weathering products

The bulk chemical composition is correlated with the mineralogical composition. Silica (SiO_2, 46–72%) and alumina (Al_2O_3, 16–31%) are the main elements present following by iron (Fe_2O_3, 2–16%) and potassium (K_2O, 0.1–8%) (Table 3). Samples from trenches 1 and 2 are enriched in potassium in agreement with the presence of potassium feldspar and/or illite. Titanium and magnesium were detected in smaller quantities (≤ 3%), revealing a low proportion of anatase. According to [38], SiO_2/Al_2O_3 ratios (~1) are characteristic of kaolinitic clays, SiO_2/Al_2O_3 ratios values of 2 indicate a mixture of kaolinite/micas or illite and samples with a ratio between 3 and 5 contain siliceous minerals. Samples T2E1 and T5A6, whose SiO_2/Al_2O_3 ratios are 4.5 and 5.5 respectively, exhibit lower LOI (< 6%) than the other samples. LOI largely represents water and organic matter. According to the XRD results, the T2E1 sample is rich in quartz and potassium feldspar with a low proportion of clay minerals.

Like T1D1 and T1A10, which contain high proportions of K_2O (6–8%), T2E1 is also characterized by a high abundance of K_2O (7%). This predicts good fusibility during the sintering process [18, 21, 39]. The high SiO_2/Al_2O_3 ratio therefore reflects the presence of siliceous minerals in addition to the silicates. Moreover, the negligible K_2O content and high SiO_2/Al_2O_3 ratio of T5A6 reflect the abundance of siliceous minerals such as quartz. T1A3, T4C1, T4C2 had the highest LOI values (15–19%) in agreement probably with the presence of swelling clays in these samples (vermiculite in sample T1A3 and smectites in whitish coloured vein in samples T4C1 and T4C2). The release of water from the structure of the swelling minerals results in higher LOI compared to non-swelling clays such as kaolinite. Smectites and vermiculites may absorb a certain amount of water from their internal surfaces and this absorption leads to the swelling of these clays following the intercalation of 0 to 4 discrete layers of water molecules in their structure [20, 40, 41]. This may explain the significant loss of ignition (LOI) values for these samples (Table 3).

The low CIA value for bedrock (56) indicates slightly weathering conditions, this being close to the CIA value of the un-weathered upper crust (50) [42]. The CIA value can be considered here as a relative measure of weathering, because many authors as Buggle et al. [43] have approved that CIA has been largely disproved mainly in samples

Table 3 Major chemical elements of representative samples

Samples	Parent rock (Mylonite)	Trench 1						Trench 2			Trench 4					Trench5					
		T1A1	T1A3	T1A8	T1A10	T1A11	T1D1	T2E1	T2E2	T2E4	T4E1	T4B1	T4C1	T4C2	T4D1	T5A1	T5A2	T5A3	T5A4	T5A5	T5A6
SiO_2	64.99	53.52	50.3	46.03	66.28	50.1	52.58	72.1	52.9	52.2	40.72	55.2	49.9	49.56	64.25	49.17	60.94	47.56	49.42	55.12	74.57
TiO_2	0.68	1.31	2.41	3.12	0.64	1.91	0.46	0.22	1.11	1.21	1.24	1.13	1.06	1.17	1.21	0.87	0.46	4.08	3.21	1.56	1.16
Al_2O_3	14.87	19.07	16.02	20.57	18.25	21.21	28.75	15.87	20.86	23.75	31.6	23.87	21.17	21.96	18.98	29.59	25.48	26.76	31.24	25.92	13.64
Fe_2O_3	4.57	8.87	12.73	16.18	3.3	11.81	1.56	1.03	12.07	9.02	11.78	7.51	6.74	9	4.31	7.6	2.41	9.47	2.97	4.52	3.45
MnO	0.07	0.18	0.31	0.18	0.05	0.14	0.01	0	0.03	0.03	0.01	0.06	0.01	0.1	0.01	0	0	0.03	0.01	0.01	0.01
MgO	2.48	2.87	2.74	0.84	0.43	1.59	0.45	0.001	0.64	0.69	0.05	0.28	0.66	1.03	0.08	0.05	0	0.12	0.07	0.19	0.01
CaO	3.43	0.07	0.06	0.05	0.03	0.03	0.03	0.05	0.04	0.04	0.02	0.05	0.21	0.07	0.1	0	0	0.01	0.01	0.03	0.01
Na_2O	3.59	0	0	0	0	0	0	0	0	0	0	0	0	0	0	0	0	0	0	0	0.47
K_2O	4.62	4.58	0.22	1.38	6.07	2.83	7.97	7.36	2.94	1.93	0.09	0.56	0.94	0.69	0.32	0.11	0.04	0.13	0.15	0.1	0.98
P_2O_5	0.38	0.23	0.17	0.38	0.07	0.27	0	0.01	0.16	0.04	0.16	0.18	0.14	0.12	0.01	0.05	0	0.15	0.07	0.04	0.04
LOI	0.64	7.64	15.03	11.27	4.87	10.11	8.2	3.36	9.26	11.1	14.34	11.16	19.18	16.31	10.74	12.57	10.66	11.7	12.85	12.52	5.66
Total	100.33	98.34	100	100	100	100	100	100	100	100	100	100	100	100	100	100	100	100	100	100	100
SiO_2/Al_2O_3	–	2.81	3.14	2.24	3.63	2.36	1.83	4.54	2.54	2.20	1.29	2.31	2.36	2.26	3.39	1.66	2.39	1.78	1.58	2.13	5.47
Alcali + Alcali-earth	–	7.70	3.33	2.45	6.58	4.59	8.46	7.41	3.65	2.69	0.17	0.95	1.82	1.89	0.51	0.16	0.04	0.29	0.24	0.33	1.48
CIA	56.09	80.40	98.28	93.50	74.95	88.12	78.23	68.17	87.50	92.34	99.65	97.51	94.85	96.65	97.84	99.63	99.84	99.48	99.49	99.50	90.33

L.O.I: loss of ignition at 1000 °C; CIA: Chemical index of alteration, Data from Mylonite [26]

containing plagioclase for evaluation of geochemical weathering indices. The CIA values of samples T1A10, T1D1 and T2E1 (68–74) (Table 3) correspond to moderately weathering material, meaning that up to 50% of the material may be disintegrated into soil. The other samples display high CIA values (80–99.8) corresponding to strong leaching of mobile elements and accumulation of immobile elements such as Al [28].

4.3 Origin of swelling clay minerals in weathering products

The loss of silica relative to alumina marks the difference between temperate climate soils and humid tropical alteration. Under conditions of intense weathering in tropical climates, kaolinite is predominant in saprolites, as noted in the study area. The clay assemblages in temperate climate soils are enriched in silica in comparison by soils formed under high rainfall conditions and consequently enriched in 2:1 clay minerals [1, 2]. The predominance of 2:1 clay minerals, vermiculite, smectites and illite, as well as their coexistence with interlayered minerals, is typical of temperate climate situations [5, 35]. In Cameroon, 2:1 minerals, and mainly smectites, are observed under dry tropical climates. Low rainfall and high temperature induce high evaporation leading to soil solutions concentrated in silica and basic cations [3, 15, 44].

The probably presence of smectite and vermiculite in the studied area in the western highland of Cameroon under a warm and humid tropical climate that usually favors kaolinite formation is peculiar. Vermiculite was observed in samples collected at the transition between the clayey layers and the plurimetric quartzo-feldspathic veins. According to Basset [11], vermiculite is found in this area in close association with chlorite and garnet, which are high-temperature minerals observed in mylonite, suggesting that it's formed through weathering of chlorite. This process is characterized by the depletion of magnesium and iron [11, 45]. Vermiculite might also be formed by fluid-mineral interactions during alteration of biotite or chlorite in response to a specific set of chemical conditions imposed on secondary plasmic microsystems [2, 11, 31]. By studying the syenitic bedrock, Njonfang et al. [25, 26] suggested that minerals as biotite and chlorite come from the following transformation (pyroxene → amphibole → biotite or chlorite → chlorite or muscovite). Under weathering conditions imposed on primary or secondary plasmic microsystems, meteoric water enters the rocks through a connected microcracks network and, biotite or chlorite may be transformed into vermiculite under fluid-mineral interactions [1, 2]. According to Velde and Meunier [2], mica or chlorite in the early weathering stage of bedrock are altered along their intergranular joints; and different polyphased mineral assemblages can be observed on the two sides of the intergranular joint: di or trioctahedral vermiculite + Fe-hydroxide + kaolinite. Also, following the time duration of fluid-interaction in the joins, a specific set of chemical conditions may be imposed, and the secondary products which have been formed in the early stages could be destabilized in the later ones [2, 13]. At Earth surface conditions, the dissolution of K-feldspar for example liberates Si, Al and K ions to form new mineral stable at the given time following three petrographical situations: (i) illite may be form if the residence time of the solution is long enough and the chemical composition of the milieu is close to equilibrium with K-feldspar, (ii) smectite, stable at lower K potential than illite, may be formed because mobile components of the immobile solution continuous to migrate by diffusion inside larger fractures, and (iii) kaolinite may be formed because it is stable at the lowest K chemical potential; here the solution is continuously diluted by meteoric water where the potential difference for the mobile component is very great and inert component as Si ions become mobile when Al remaining inert [1, 2]. Overall, the appearances of vermiculite and smectite in the studied area are transitional. According to Wang et al. [46], different clay minerals present in clayey raw materials may influence the behaviour of the finished products depending on their respective concentrations therein. The starting materials must contain kaolinite and illite as base clay minerals; other clay minerals can be considered impurities or additives, and their total content must be less than 20 wt% [16, 46, 47].

4.4 Potential in terracotta products

The XRD results, reported in a triangular diagram according to [47] (Fig. 7) indicate 2 clusters: clayey materials from trenches 1 and 2 are concentrated in the inner triangle, reflecting an intermediate composition between the three poles, and clayey materials from trenches 4 and 5 with a higher proportion of clay minerals. According to Fiori et al. [47], the zone of the inner triangle corresponds to materials containing more than 50% of the clay components, generally for "plastic" red bodies. Clays from trenches 1, 2 and 4 can be most suitable for the manufacture of sandstones or red stoneware, and those from trench 5 may be used for ceramic floor tile with a moderate white color. Furthermore, Ngun et al. [48] suggested that clayey materials containing more than 50% clay minerals can be used for the manufacture of white products and porous products. Clay mineralogy plays an important role in the ceramic process and kaolinite being a major component of the raw materials, is one of the most widely used because of its high fusion temperature and white

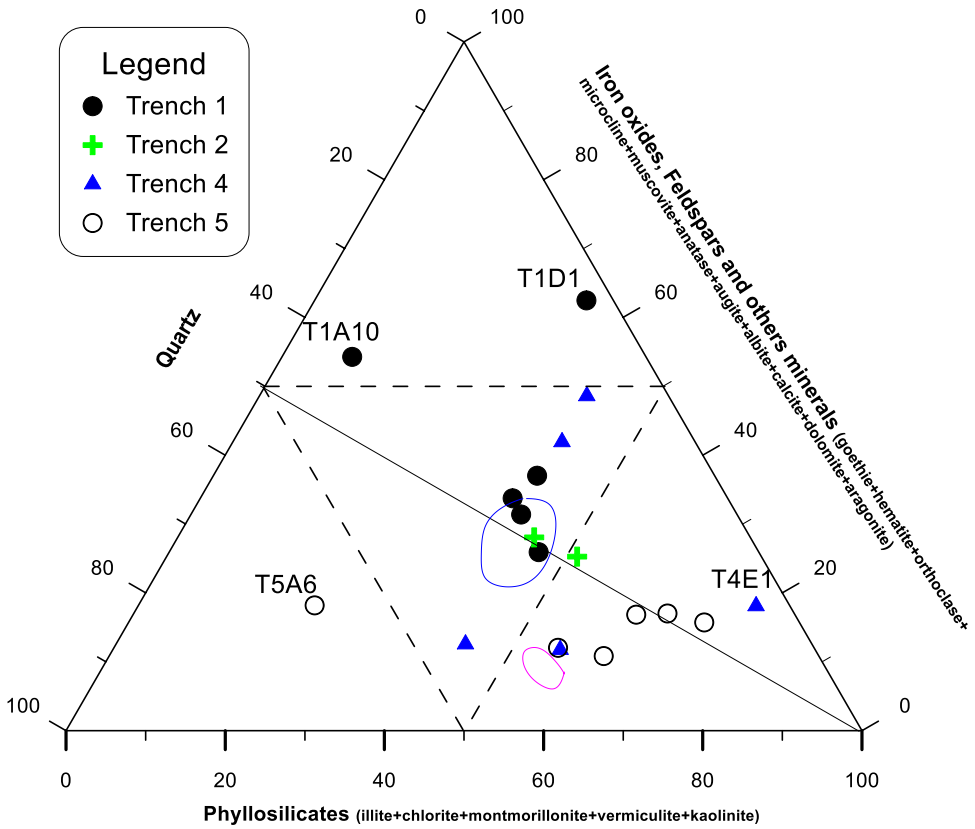

Fig. 7 Triangular diagram Quartz/Iron oxide + Feldspars + Other minerals/Clay minerals for all clayey material studied, according to [47]

color characteristics. Montmorillonite and vermiculite may provide greater plasticity in ceramic process, but causes problems (cracks) in fired products. Illite (micaceous mineral) act as a fluxing agent to guaranty faster frittage [18, 40].

The Fabbri and Fiori diagram [49] (Fig. 8) is used to compare the Njimom clayey materials with reference raw clayey materials used in the sandstone tile production industries (Italy, Germany, England and France) [48]. Clayey materials from trench 5 and T4D1 from trench 4 can be used for the production of white sandstone tiles according to [50]. However, the color of sandstones is strongly dependent on the proportion of iron oxides [17, 39, 48]. For example, T1D1, which has a low content of Fe_2O_3 (1.5%), could serve as an additive to decrease the amount of iron.

According to Murray [16, 17], 3 groups can be distinguished based on the Fe_2O_3 content of the raw clayey material: Fe_2O_3 clays at 5% give red products, those with Fe_2O_3 content between 1 and 5% give bronze colour products, and clays with Fe_2O_3 content less than 1% give white colour products. Samples from trenches 2 and 4 can be used for the production of red sandstone tiles (II). Samples of trench 2 can also be used for the manufacture of porous products such as tiles and bricks and semi-vitrified tiles, as well as clays of trench 1 whose plotted points appear in domains III and IV, representing those used in Italy for the manufacture of "cottoforte" type tiles (semi-vitrified tiles with a double firing stage) and "majolica" type tiles (Italian equivalent of earthenware), respectively. Sample T5A3, which was rich in titanium oxide (4%) and iron oxide (9%), could give a peculiar color to the fired product.

5 Conclusion

The weathering products from the mylonite of Njimom were investigated to determine the clay mineralogy and the potential of samples in terracotta production. The main results are as follows:

The mineralogy observed in the weathering products of Njimom include quartz, feldspars, muscovite, anatase, hematite and goethite as non-clay minerals followed by kaolinite and illite as the main clay minerals. Reporting in the XRD and FTIR results interpretations, the 2:1 swelling clay minerals (vermiculite, smectite) may be present in the milieu mainly in the contact between weathering materials and the quartzo-feldspatic veins observed, despite the climatic conditions prevail (humid tropical zone, high rainfall), leading to conclude of the transitional appearances of that 2:1 clay minerals.

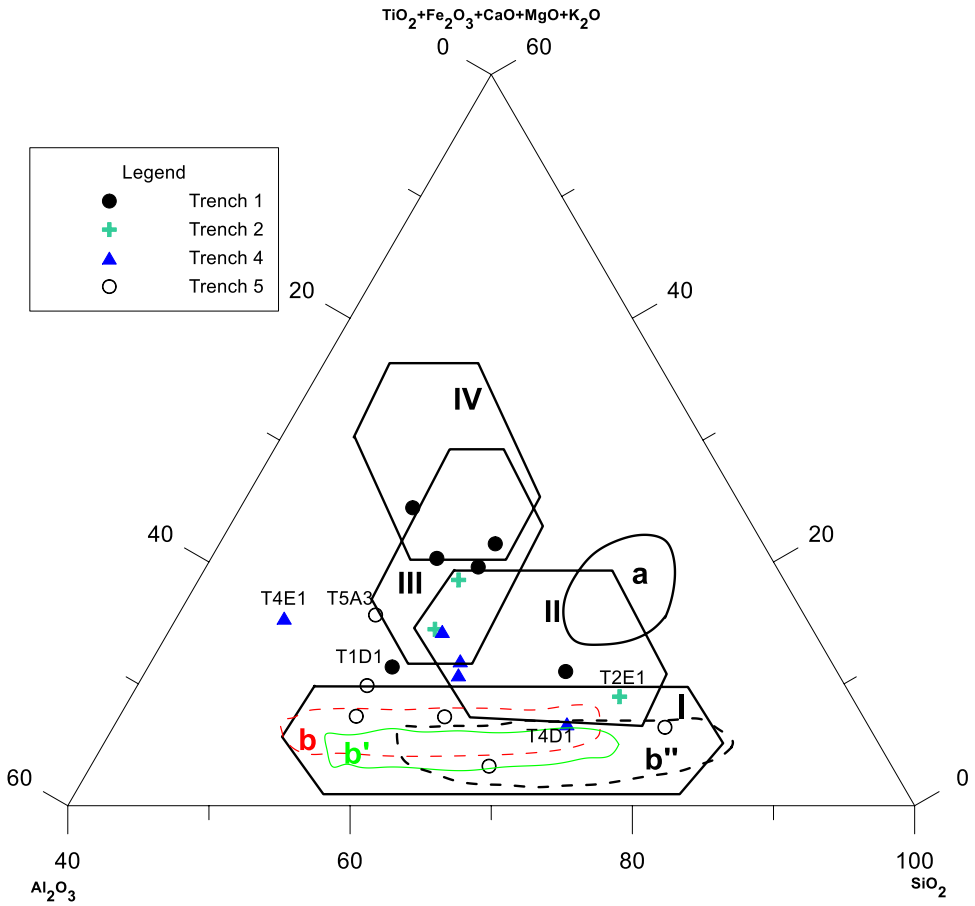

Fig. 8 Synthetic triangular diagram based on the work of [47, 48, 50] for Njimom clays: SiO_2/Al_2O_3/other oxides. Area II and a = red sandstone tile (Italy); b, b ', b' '= white sandstone tile of the German, English and French industries respectively compatible with domain I. Domains III and IV = "Cottoforte" and "Majolica" porous tiles, respectively

With the present clay minerals (kaolinite, illite) in the weathering products, these later can be adjusted in order to produce common terra cotta. Samples representative of trenches 1 to 4 can be used for the manufacture of solid bricks, while samples for trench 5 can be used for the production of white stoneware tiles. The quality of these bricks would improve if a mixture of materials from these trenches was made.

Acknowledgements The authors are grateful to the Belgian Government for the financial support given to this work through the Académie de Recherche et d'Enseignement Supérieur-Commission de la Coopération au Développement (ARES-CCD) within the framework of the Project entitled *Valorisation des Argiles de Foumban* (PRD 2013-2018).

Author contributions A.N. Nzeukou: Conceptualization, methodology, writing—original draft preparation, writing—reviewing and editing. D. Tsozué: Methodology, writing—reviewing and editing, visualization. I.Y. Bomeni: Investigation, formal analysis, writing—reviewing. J.R. Mache: Writing—reviewing, investigation, formal analysis, funding acquisition. M.R. Kwopnang: Data curation, investigation, formal analysis, validation, software. N. Fagel: Writing—reviewing and editing, methodology, supervision, funding acquisition, project administration.

Data availability The datasets generated during and/or analyzed during the current study are available from the corresponding author on reasonable request.

Declarations

Competing interests The authors declare no competing interests.

References

1. Wilson MJ. The origin and formation of clay minerals in soils: past, present and future perspectives. Clay Miner. 1999;34:7–25. https://doi.org/10.1180/000985599545957.
2. Velde B, Meunier A. The origin of clay minerals in soils and weathered rocks. Berlin: Springer; 2008.
3. Nguetnkam JP, Kamga R, Villiéras F, Ekodeck GE, Yvon J. Altération différentielle du granite en zone tropicale. Exemple de deux séquences étudiées au Cameroun (Afrique centrale). Comptes Rendus Geo. 2008;340:451–61. https://doi.org/10.1016/j.crte.2008.02.002.
4. Azam S. Influence of mineralogy on swelling and consolidation of soils in eastern Saudi Arabia. Can Geotech J. 2003;40:964–75. https://doi.org/10.1139/t03-047.
5. April HR, Hluchy MM, Newton RM. The nature of vermiculite in Adirondack soils and till. Clays Clays Min. 1986;34:549–56. https://doi.org/10.1346/CCMN.1986.0340508.
6. Hanlie H, Fang Qian WC, Gong N, Zhao L. Constraints of parent magma on altered clay minerals: a case study on the ashes near the Permin-Triassic Boundary in Xinmin Section, Guizhou Province. J China Univ. 2017;42:161–72.
7. Schulze DG. Mineral components of the soil clay fraction. In: Encyclopedia of Soils in the Environment (Second Edition), Elsevier, 2023;4: pp.109–120.
8. Ross GJ, Kodama H. Experimental alteration of a chlorite into regularly interstratified chlorite-vermiculite by chemical oxidation. Clays Clay Min. 1976;24:183–90. https://doi.org/10.1346/CCMN.1976.0240406.
9. Curtin D, Smillie GW. Composition and origin of smectite in soils derived from basalt in Northern Ireland. Clays Clay Min. 1981;29:277–84. https://doi.org/10.1346/CCMN.1981.0290405.
10. Srodon J. Nature of mixed-layer clays and mechanisms of their formation and alteration. Annu Earth Planet Sci. 1999;27:19–53. https://doi.org/10.1146/annurev.earth.27.1.19.
11. Wypych F, Rilton A. de Freitas. Chapter 1 - Clay minerals: Classification, structure, and properties. In: Clay Minerals and Synthetic Analogous as Emulsifiers of Pickering Emulsions, Developments in Clay Science, 2022: 10: pp 3–35.
12. Bassett WA. The geology of vermiculite occurrences. Clays Clay Min. 1961;10:61–9.
13. Courshesne F, Chapdelaine C, Munro L. The origin of smectite in the soil of the Kruger 2 archaeological site, Brompton (Québec), Canada. Geoarchaeology. 2019;34:783–96. https://doi.org/10.1002/gea.21751.
14. Środoń, J. Chapter 2–2—Identification and quantitative analysis of clay minerals. In Handbook of Clay Science, Developments in Clay Science, 2013; 5: pp 25–49. https://doi.org/10.1016/B978-0-08-098259-5.00004-4
15. Tsozué D, Basga SD, Nzeukou AN. Spatial variation of soil weathering processes in the tropical high reliefs of Cameroon (Central Africa). Eurasian J Soil Sci. 2020;9(2):92–104. https://doi.org/10.18393/ejss.659830.
16. Reeves GM, Sims I, Cripps C. Clay materials used in construction. London: Geological Society, London, Engineering Geology Special Publication; 2006.
17. Murray HH. Applied clay mineralogy Volume 2: Occurrences, Processing and Applications of Kaolins, Bentonites, Palygorskite-sepiolite, and Common Clays. Amsterdam: Elsevier; 2007.
18. Dondi M, Raimondo M, Zanelli C. Clays and bodies for ceramic tiles: reappraisal and technological classification. Appl Clay Sci. 2014;96:91–109. https://doi.org/10.1016/j.clay.2014.01.013.
19. Nzeukou Nzeugang A, Medjo Eko R, Fagel N, Kamgang Kabeyene V, Njoya A, Balo Madi A, Mache J-R, Melo CU. Characterization of clay deposits of Nanga-Eboko (Central Cameroon): suitability in the production of building materials. Clay Min. 2013;48:655–62. https://doi.org/10.1180/claymin.2013.048.4.18.
20. Mache JR, Signing P, Mbey JA, Razafitianamaharavo A, Njopwouo D, Fagel N. Mineralogical and physico-chemical characteristics of Cameroonian Smectitic clays after treatment with low sulfuric acid. Clays Min. 2016. https://doi.org/10.1180/claymin.2015.050.5.08.
21. Ndjigui PD, Mbey JA, Nzeugang NA. Mineralogical, physical and mechanical features of ceramic products of the alluvial clastic clays from the Ngog-Lituba region, Southern Cameroon. J Buil Eng. 2016;5:151–7. https://doi.org/10.1016/j.jobe.2015.11.009.
22. Nkoumbou C, Njoya A, Njoya D, Grosbois C, Njopwouo D, Yvon J, Martin F. Kaolin from Mayouom (Western Cameroon): industrial suitability evaluation. Appl Clay Sci. 2009;43:118–24. https://doi.org/10.1016/j.clay.2008.07.019.
23. Njoya A, Nkoumbou C, Grosbois C, Njopwouo D, Njoya D, Courtin-Nomade A, Yvon J, Martin F. Genesis of Mayouom kaolin deposit (western Cameroon). Appl Clay Sci. 2006;32:125–40. https://doi.org/10.1016/j.clay.2005.11.005.
24. Bomeni I, Kenmoe MR, Nzeugang Nzeukou A, Pirard E, Wouatong ASL, Fagel N. Application of geostatistical methods to estimate the mineral contents in the alluvial clay deposit, Monoum plain, West Cameroon. Arab J Geosci. 2022;15:1774. https://doi.org/10.1007/s12517-022-11064-8.
25. Njonfang E, Moreau C, Tchoua FM. The Foumban-Bankim mylonitic band, west-Cameroon. A HT-MP shear zone. Earth Plan Sci. 1998;327:735–41. https://doi.org/10.1016/S1251-8050(99)80044-5.
26. Njonfang E, Ngako V, Kwekam M, Affaton P. Les orthogneiss calco-alcalins de Foumban-Bankim : témoins d'une zone interne de mage active panafricaine en cisaillement. CR Geosci. 2006;338:606–16. https://doi.org/10.1016/j.crte.2006.03.016.
27. Moore DM, Reynolds RCJ. X-Ray Diffraction and the identification and analysis of clay minerals. New York: Oxford University Press; 1989.
28. Nesbitt HW, Young GM. Early Proterozoic climates and plate motions inferred from major element chemistry of lutites. Nature. 1982;279:715–7. https://doi.org/10.1038/299715a.
29. Craw D. Ferrous-Iron-Bearing Vermiculite-Smectite series formed during alteration of chlorite to kaolinite, Otago Schist, New Zealand. Clay Min. 1984;19:509–20. https://doi.org/10.1180/claymin.1984.019.4.01.
30. Tomanec R, Popov S, Vucinic D, Lazic P. Vermiculite from Kopaonik (Yugoslavia) characterization and processing. Fizykochemiczne Problemy Mineralurgii. 1997;31:247–54.

31. Proust D. Supergene alteration of metamorphic chlorite in an amphibole from massif central. France Clay Min. 1982;17:159–73. https://doi.org/10.1180/claymin.1982.017.2.01.
32. Madejova J. FTIR techniques in clay mineral studies. Vibra Spectros. 2003;31:1–10. https://doi.org/10.1016/S0924-2031(02)00065-6.
33. Sirbu-Radasanu DS, Huzum R, Dumitras DG, Stan CO. Mineralogical and geochemical implications of weathering processes responsible for soil generation in Mănăila Alpine area (Tulghes 3 Unit-Eastern Carpathians). Minerals. 2022;12:1161. https://doi.org/10.3390/min12091161.
34. Chukanov NV. Infrared spectra of mineral species. Extended library. Dordrecht: Springer; 2013.
35. Worasith N, Goodman BA, Neampan J, Jeyachoke N, Thiravetyan P. Characterization of modified kaolin from the Ranong deposit Thailand by XRD, XRF, SEM, FTIR and EPR techniques. Clay Min. 2011;46:539–59. https://doi.org/10.1180/claymin.2011.046.4.539.
36. Taboada T, Garcia C. Smectite formation produced by weathering in a coarse granite saprolite in Galicia NW Spain. CATENA. 1999;35:281–90. https://doi.org/10.1016/S0341-8162(98)00107-6.
37. Borchardt G. Smectites. In: Dixon JB, Weed SB, Eds. Minerals in Soil Environments.2ed. Soil Science Society of America, Inc; 1989, 675–727. https://doi.org/10.2136/sssabookser1
38. Elfil H, Srasra E, Dogguy M. Caractérisations physico-chimiques de certaines argiles utilisées dans l'industrie céramique. J Thermal Anal. 1995;44:663–83. https://doi.org/10.1007/BF02636285.
39. Ben M'barek-Jemaï M, Ali S, Imed BS, Lassaad BA, Samir B, Joelle D. Geological and technological characterization of the Late Jurassic-Early Cretaceous clay deposits for ceramic industry. J Afr Earth Sci. 2017;129:282. https://doi.org/10.1016/j.jafrearsci.2017.01.019.
40. Christidis GE. Advances in the characterization of industrial clays, EMU Notes in mineralogy, 9. European mineralogical Union, Mineralogical Society of Great Britain and Ireland. 2011
41. Laird DA. Influence of layer charge on swelling of smectites. Appl Clay Sci. 2006;34:74–87. https://doi.org/10.1016/j.clay.2006.01.009.
42. Xu Z, Tang C, Chen L, Xiao P, Liu H, Zeng H, Duan M. Petrography and geochemistry of Late Cretaceous clastic rocks in the northern Songliao Basin, north-eastern China: implications for provenance and weathering. Geol J. 2023;58:1–15. https://doi.org/10.1002/gj.4730.
43. Buggle B, Glaser B, Hambach U, Gerasimenko N, Markovi SN. Evaluation of geochemical weathering indices in loess-paleosol studies for an overview of different indices. Quat Int. 2011;240:12–21. https://doi.org/10.1016/j.quaint.2010.07.019.
44. Tsozué D, Nzeugang Nzeukou A, Pagna Kagonbé B, Balo Madi A, Mache JR, Bitom DL, Fagel N. Genesis and assessment of clay materials suitability for earthenware production in northern Cameroon. Arab J Geosci. 2022;15:1376. https://doi.org/10.1007/s12517-022-10603-7.
45. Johnson LJ. Occurrence of regularly interstratified Chlorite-Vermiculite as a weathering product of Chlorite in a soil. The Ameri Mineralo. 1964;49:556–72.
46. Wang SL, Gainey IDR, Mackinnon C, Allen Y, Gu Y, Xi Y. Thermal behaviors of clay minerals as key components and additives for fired brick properties: a review. J Build Eng. 2023;66:105802. https://doi.org/10.1016/j.jobe.2022.105802.
47. Fiori C, Fabbri B, Donati F, Venturi I. Mineralogical composition of the clay bodies used in the Italian tile industry. Appl Clay Sci. 1989;4:461–73. https://doi.org/10.1016/0169-1317(89)90023-9.
48. Ngun BK, Mohamad H, Sulaiman SK, Okada K, Ahmad ZA. Some ceramic properties of clays from central Cambodia. Appl Clay Sci. 2011;53:33–41. https://doi.org/10.1016/j.clay.2011.04.017.
49. Fabbri B, Fiori C. Clays and complementary raw materials for stone ware tiles. Mineralo Pertrogra Acta. 1985;29A:535–45.
50. Strazzera B, Dondi M, Maesigli M. Composition and ceramic properties of Tertiary clays from southern Sardinia (Italy). Appl clay Sci. 1997;12:247–66. https://doi.org/10.1016/S0169-1317(97)00010-0.
51. Cirotteau A, Leroy B, Weecksteen G. Carte géologique de reconnaissance du Cameroun. Douala-Est. NB32SE-E29, 1 :500 000. Direction Mines et Géologie du Cameroun. 1957.